

Deep level transient spectroscopic study of neutron-irradiated *n*-type 6H-SiC

X. D. Chen,^{a)} S. Fung, C. C. Ling, and C. D. Beling

Department of Physics, The University of Hong Kong, Pokfulam Road, Hong Kong, People's Republic of China

M. Gong^{b)}

Department of Physics, Sichuan University, Chengdu, Sichuan 610064, People's Republic of China

(Received 20 March 2003; accepted 12 June 2003)

Deep level transient spectroscopy has been employed to study the deep level defects introduced in *n*-type 6H-SiC after neutron irradiation. Deep levels situated at $E_C-0.23$, $E_C-0.36/0.44$, $E_C-0.50$, and $E_C-0.62/0.68$ eV have been detected in the temperature range of 100–450 K, which have been identified with the previously reported deep levels $ED1$, E_1/E_2 , E_i , and Z_1/Z_2 , respectively. Thermal annealing studies of these deep levels reveal that $ED1$ and E_i anneal at a temperature below 350 °C, the Z_1/Z_2 levels anneal out at 900 °C, while the intensity of the E_1/E_2 peaks is increased with annealing temperature, reaching a maximum at about 500–750 °C, and finally annealing out at 1400 °C. The possible nature of the deep levels $ED1$, E_1/E_2 , E_i , and Z_1/Z_2 are discussed in the context of their annealing behavior. Upon further annealing at 1600 °C, four deep levels labeled $NE1$ at $E_C-0.44$ eV, $NE2$ at $E_C-0.53$ eV, $NE3$ at $E_C-0.64$ eV, and $NE4$ at $E_C-0.68$ eV are produced. Evidence is given that these levels are different in their origin to E_1/E_2 and Z_1/Z_2 . © 2003 American Institute of Physics. [DOI: 10.1063/1.1598629]

I. INTRODUCTION

Silicon carbide (SiC) is a wide band-gap semiconductor material having unique physical and electronic properties for high-temperature, high-power, and high-frequency electronic device applications.¹ In modern SiC device technology, electron irradiation and ion implantation are usually employed for the purposes of carrier lifetime control and creating doped layers. It is always found that irradiation-induced defects remain in the operating area of the device even after the annealing procedure.^{2–4} In past years, deep level defects induced by particle irradiation or ion implantation in SiC have been extensively studied by capacitance transient techniques such as deep level transient spectroscopy (DLTS).^{2–10} Deep levels at $E_C-0.6-0.7$ eV (termed Z_1/Z_2) have been reported to be persistent even after thermal annealing at 1700 °C and are generated either by irradiation with high-energy electrons or by implantation of ions.^{2–4} However, recent DLTS studies of the thermal annealing behavior of the Z_1/Z_2 levels have shown that these levels almost disappear with postirradiation annealing temperatures below 1000 °C.^{6,7} Another important grouping of deep levels are those found at $E_C-0.36$ and $E_C-0.44$ eV (usually termed E_1/E_2). These peaks are normally seen in the DLTS spectra of electron-irradiated 6H-SiC.^{4–8} However, in the studies of He implanted⁴ and deuterium implanted⁷ *n*-type 6H-SiC, E_1/E_2 are not clearly detectable in as-irradiated samples, but they become so after thermal annealings of 430 °C⁴ and

800 °C,⁷ respectively. E_1/E_2 appears to be the most stable of defect centers, only annealing out at temperatures above 1200 °C.^{4–8} In addition to Z_1/Z_2 and E_1/E_2 there is usually also seen in electron-irradiated material a less prominent peak labeled E_i at $\sim E_C-0.50$ eV.^{4–8} The atomic structures of the E_1/E_2 , Z_1/Z_2 , and E_i levels have attracted a great deal of discussion but have not yet been unambiguously clarified.

Nuclear transmutation doping (NTD) has been shown to be a promising technique for doping the material with phosphorus (P) donor.^{11,12} This technology is based on the capture of a thermal neutron of ^{30}Si by the reaction [$^{30}\text{Si}(n, \gamma) - ^{31}\text{Si}$] and the subsequent β^- decay which forms the dopant ^{31}P . However, the defects introduced by (n, γ) recoil and by fast neutrons can act as compensation centers and thus influence the electrical properties of the material.¹³ Thus, there is a need to identify and to understand the defects introduced by neutron irradiation. Neutron irradiation-induced deep levels labeled $H1$, $H2$, $H3$, and $E2$ in 3C-SiC have been reported by Nagesh *et al.*^{13,14} In the case of neutron irradiated 6H-SiC, it was reported that neutron-irradiation defects were generated homogeneously throughout the crystal.¹⁵ Defect centers introduced by neutron radiation have been investigated using electron paramagnetic resonance (EPR),¹⁶ positron annihilation spectroscopy (PAS),¹⁷ magnetic circular dichroism of the absorption (MCDA) and MCDA detected EPR (MCDA-EPR),¹⁸ but this kind of study using DLTS is still lacking. DLTS is one of the most direct techniques for the determination of energy states of deep level defects. In the present report, deep level defects formed in *n*-type 6H-SiC irradiated with different doses of neutron have been studied by the DLTS technique. The nature of the observed

^{a)} Author to whom correspondence should be addressed; electronic-mail: chenxa@hkusua.hku.hk

^{b)} Also at: International Center for Materials Physics, Chinese Academy of Science, Shenyang, 110015, People's Republic of China.

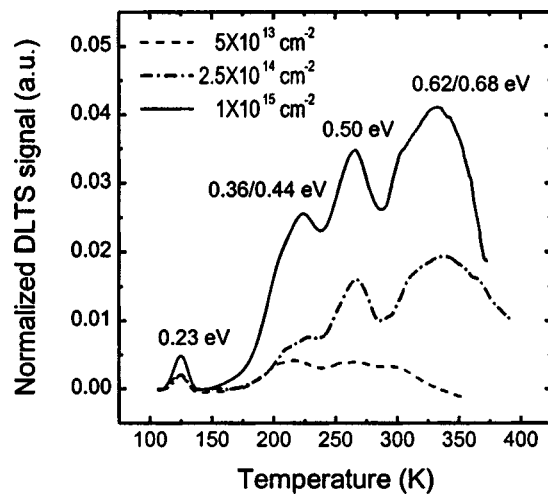


FIG. 1. Normalized DLTS spectra for n -type 6H-SiC irradiated with neutrons to doses of $5 \times 10^{13} \text{ n/cm}^2$, $2.5 \times 10^{14} \text{ n/cm}^2$, and $1 \times 10^{15} \text{ n/cm}^2$. A rate window of 6.82 ms was used in the measurements.

defect levels has been discussed according to their observed thermal annealing behavior.

II. EXPERIMENT

The starting n -type 6H-SiC samples used in this experiment were purchased from CREE Research Inc. in the form of a $5\text{-}\mu\text{m}$ -thick nitrogen doped (0001) oriented epitaxial layer grown on n^+ -type 6H-SiC substrate. The nitrogen donor concentrations were 1×10^{16} and $8 \times 10^{17} \text{ cm}^{-3}$ in the epitaxial layer and the substrate, respectively. The samples were rinsed in boiling acetone, ethanol, and de-ionized water, and were then chemically treated in 10% hydrofluoric acid solution to remove the oxidation layer. Large area ohmic contacts were made by evaporating Al on the backside of the samples followed by a 5 min annealing process at 900°C in pure nitrogen gas.

The samples were irradiated with neutrons at room temperature to doses of 5.1×10^{13} , 2.5×10^{14} , and $1.0 \times 10^{15} \text{ n/cm}^2$, respectively. The flux ratio of fast neutrons to thermal neutrons was around 30%. Isochronal thermal annealing of the irradiated samples was carried out in an atmosphere of nitrogen gas at temperatures between 100 and

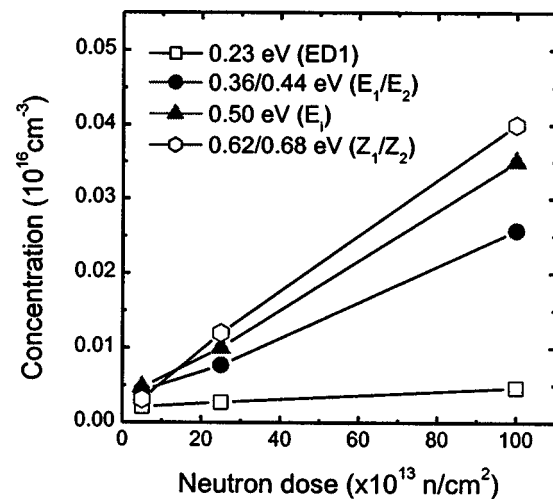


FIG. 2. Concentration of the observed deep levels as a function of the neutron dose for the energy levels 0.23, 0.36/0.44, 0.50, and 0.62/0.68 eV. The lines joining the points are only for visual guidance.

1100°C for 30 min. Higher temperature annealing at 1200 , 1400 , and 1600°C were performed for 30 min in pure argon gas. Schottky contacts for DLTS measurement were prepared by depositing gold dots of 0.6 mm diameter by thermal evaporation on the surface of epitaxial layer.

The DLTS system used in the present work has been described elsewhere.¹⁹ These measurements were carried out by applying a reverse bias of $V_r = -6 \text{ V}$, with a forward filling pulse of $V_p = 6 \text{ V}$. DLTS spectra were taken in the range of $100\text{--}450 \text{ K}$. The trap energy levels and capture cross sections were determined from the slope and the intercept of the Arrhenius plots using the equation $e_n/T^2 = \gamma_n \sigma_n \exp\{-(E_C - E_t)/kT\}$ where e_n is the rate of emission from the trap to the conduction band, γ_n is a constant comprised of the temperature independent terms of the density of states and electron thermal velocity, σ_n is the capture cross section, and $(E_C - E_t)$ is the deep level activation energy. The trap concentration was evaluated from the peak heights of the DLTS signal using the procedure described in Ref. 20. In the calculations, the defect capture cross sections were assumed to be temperature independent.

TABLE I. Energy levels ($E_C - E_t$), capture cross sections (σ_n), and production rates of the deep levels determined using the DLTS data of the neutron irradiated n -type 6H-SiC samples.

Present DLTS study on neutron irradiated samples			Previously reported deep level defects in n -type 6H-SiC after irradiation or implantation of particles		
$E_C - E_t$ (eV)	σ_n (cm^2)	Production rate (cm^{-1})	Electron irradiated	Proton and deuterium irradiated	He implanted
0.23	$\sim 10^{-15}$	~ 0.02	ED1 (0.27 eV) [Ref. 6]		
0.36/0.44	$\sim 10^{-14}$	$\sim 0.4/0.5$	E_1/E_2 (0.38/0.44 eV), $\sigma \sim 10^{-14} \text{ cm}^{-2}$ [Ref. 5]	0.34/0.41 eV, [Ref. 7] 0.36/0.40 eV, $\sigma \sim 10^{-15} \text{ cm}^{-2}$ [Ref. 8]	E_1/E_2 (0.39–0.43 eV), $\sigma \sim 10^{-14} \text{ cm}^{-2}$ [Ref. 4]
0.50	$\sim 10^{-15}$	~ 0.7	0.51 eV, [Ref. 7] E_i (0.51 eV), $\sigma \sim 10^{-15} \text{ cm}^{-2}$ [Ref. 5]	0.51 eV ^d	RD5 (0.43–0.47 eV), $\sigma \sim 10^{-15} \text{ cm}^{-2}$ [Ref. 4]
0.62/0.68	$\sim 10^{-16}$	$\sim 0.6/0.7$	Z_1/Z_2 , $\sigma \sim 10^{-16}\text{--}10^{-17} \text{ cm}^{-2}$ [Ref. 5]	0.62/0.64 eV, [Ref. 7] 0.7 eV, $\sigma \sim 10^{-15} \text{ cm}^{-2}$ [Ref. 8]	Z_1/Z_2 (0.65–0.72/0.58–0.63 eV), $\sigma \sim 10^{-15}\text{--}10^{-14} \text{ cm}^{-2}$ [Ref. 4]

III. RESULTS

Figure 1 shows the DLTS spectra of the as-irradiated *n*-type 6H-SiC samples with neutron doses of 5.1×10^{13} , 2.5×10^{14} , and 1.0×10^{15} n/cm², respectively. Six major peaks are observed in these spectra having activation energies of $E_C - 0.23$, $E_C - 0.36$, $E_C - 0.44$, $E_C - 0.50$, $E_C - 0.62$, and $E_C - 0.68$ eV, the closely spaced 0.36/0.44 eV levels, and 0.62/0.68 eV levels overlapping with each other to give broad peaks that can only just be decomposed. DLTS measurements performed on un-irradiated Schottky contacted epitaxial layer control samples did not reveal any deep levels with concentration above $\sim 10^{13}$ cm⁻³, indicating that all the observed defect levels are neutron induced.

The fluence dependence of the defect concentrations evaluated using the present DLTS data is shown in Fig. 2. As can be seen, the observed deep levels depend proportionally on neutron dose, again indicating that they are neutron irradiation introduced. The energy levels, capture cross sections and introduction rates of the deep levels are summarized in Table I. It was reported by individual groups that in *n*-type 6H-SiC, deep level defects labeled *ED1*, E_1/E_2 , E_i (or *RD5*) and Z_1/Z_2 are induced by electron irradiation,⁵⁻⁷ proton,⁸ deuterium,⁷ or He implantation.^{4,9,10} The activation energies and capture cross sections of these deep level defects as reported by these other workers are also listed in Table I for reference. Good agreement is seen between the parameters of the present neutron irradiation induced defects and those reported from the previous studies. Thus, the present observed deep levels $E_C - 0.23$, $E_C - 0.36/0.44$, $E_C - 0.50$, and $E_C - 0.62/0.68$ eV are believed to be the levels *ED1*, E_1/E_2 , E_i (or *RD5*), and Z_1/Z_2 , respectively, and the same nomenclature is retained in this study.

As shown in the DLTS spectrum of the 2.5×10^{14} n/cm² dose as-irradiated sample in Fig. 1, it can be seen that the amplitude ratio of the E_1/E_2 peak to the E_i peak is roughly 0.4/1 and referencing the peak height of E_1/E_2 to Z_1/Z_2 gives a similar ratio. These relative intensities are quite different from those reported in the electron-irradiated 6H-SiC material where one typically finds the E_i and Z_1/Z_2 peaks an order of magnitude less in intensity than E_1/E_2 .⁵⁻⁷ The increased importance E_i and of Z_1/Z_2 peaks in the neutron-irradiated material is consistent with the as-irradiated samples being implanted by heavy particles (like deuterium⁷ and He^{4,10}).

To investigate the thermal annealing behavior of the observed deep level defects, 100–1600 °C isochronal annealing was performed on the as-irradiated samples with each of the annealing steps lasting for 30 min. Figure 3 shows some of the typical DLTS spectra of the neutron-irradiated samples annealed at temperatures between 200 and 1400 °C, from which the extinction of the deep levels *ED1*, E_1/E_2 , E_i , and Z_1/Z_2 during the annealing process are clearly seen. Isochronal annealing curves for the normalized DLTS signal intensities of *ED1*, E_1/E_2 , E_i , and Z_1/Z_2 are shown in Fig. 4 from which it may be seen that *ED1* and E_i both anneal out below 350 °C. On the other hand, the level E_1/E_2 increases with annealing temperature, reaching a maximum at temperature of ~ 500 °C, thereafter dropping and reaching

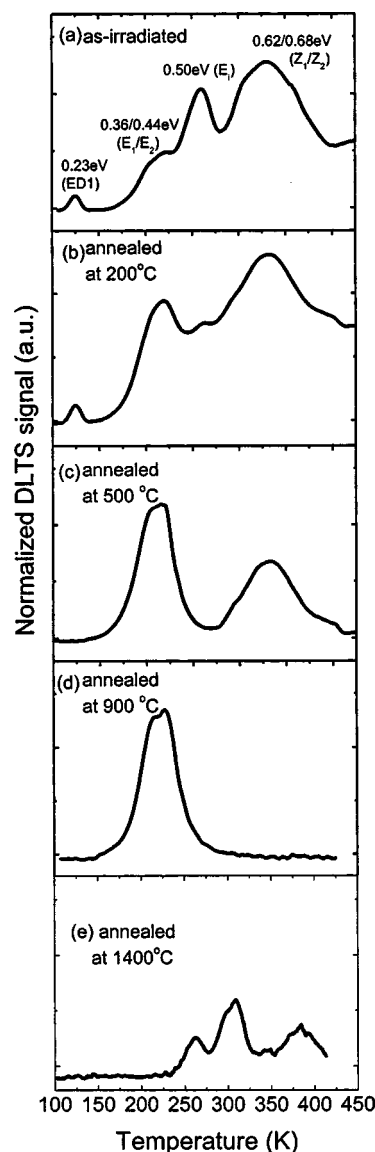


FIG. 3. Normalized DLTS spectra for *n*-type 6H-SiC irradiated with neutron to dose 2.5×10^{14} n/cm² with subsequent annealing at 200 °C (b), 500 °C (c), 900 °C (d), and 1400 °C (e), respectively.

the DLTS signal limit ($\sim 10^{12}$ cm⁻³) above 1400 °C. For the case of Z_1/Z_2 , the intensity decreases slightly with sample annealed up to 500 °C and then undergoes a drastic decrease at ~ 750 °C, finally falling below the DLTS signal limit at 900 °C.

Annealing at temperatures beyond 1400 °C produces some interesting results. Figure 5 shows the DLTS spectra of the 500 and the 1600 °C annealed neutron-irradiated *n*-type 6H-SiC samples. A 1600 °C annealing of un-irradiated control sample was also performed with the corresponding DLTS spectrum also included in Fig. 5. For the neutron irradiated sample, although all the deep levels *ED1*, E_1/E_2 , E_i , and Z_1/Z_2 have already annealed out at the annealing temperature of 1400 °C, four additional DLTS peaks (denoted by *NE1–NE4*) are observed after the 1600 °C annealing. Arrhenius plots for the *NE1–NE4* deep levels are shown in Fig. 6. The activation energies and capture cross sections of the *NE1–NE4* levels are summarized in Table II. Moreover,

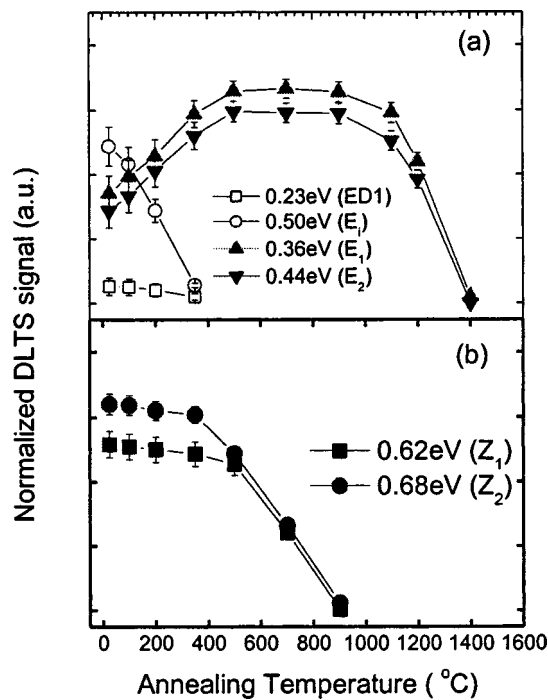


FIG. 4. Peak intensity as a function of annealing temperature for the deep levels (a) 0.23, 0.36/0.44, and 0.50 eV; and (b) 0.62/0.68 eV measured from the sample irradiated with neutron to dose of 2.5×10^{14} n/cm².

these four peaks can also be seen in the DLTS spectrum of the 1600 °C annealed nonirradiated sample, although the peak intensities are much lower than those of the 1600 °C annealed neutron-irradiated sample.

IV. DISCUSSION

A. E_D level

It can be seen in Fig. 1 that the neutron induced level ($E_C - 0.23$ eV) level is a relatively weak DLTS peak. Its activation energy is close to that of E_D ($E_C - 0.27$ eV),

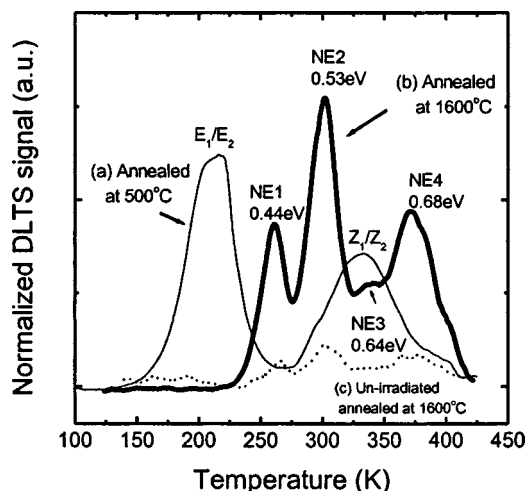


FIG. 5. Normalized DLTS spectra for *n*-type 6H-SiC irradiated with neutron to dose 2.5×10^{14} n/cm² with subsequent annealing at 500 °C (a), 1600 °C (b), and un-irradiated control sample with annealing at 1600 °C (c), respectively. A rate window of 6.82 ms was used in the measurements.

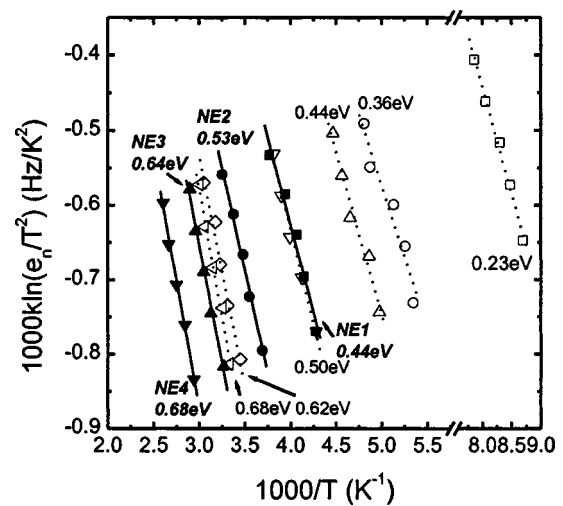


FIG. 6. Arrhenius plots of the emission rates $1000 \ln(e_n/T^2)$ vs reciprocal temperature for as-neutron-irradiated *n*-type 6H-SiC to dose of 2.5×10^{14} n/cm² (open scatters and dotted lines) and for irradiated sample with subsequent annealing at 1600 °C (closed scatters and solid lines), respectively. Here k is the Boltzmann constant and e_n is the emission rate corresponding to different rate windows.

which was previously found in electron-irradiated 6H-SiC samples.⁶ Similar to the annealing temperature of E_D (~ 300 °C), the deep level $E_C - 0.23$ eV also anneals out at a relatively low temperature (< 350 °C). Because of its low annealing temperature, Gong *et al.*⁶ suggested that E_D was possibly related to an interstitial defect as such sites have a relatively low migration energy.

B. E_i level

The $E_C - 0.50$ eV level in the present neutron-irradiated experiment is very close to the E_i deep level found in the electron-irradiated at $E_C - 0.51$ eV^{5,7} and the level $RD5$ (at $E_C - 0.5$ eV) found in He implanted 6H-SiC materials.⁴ Aboelfotoh and Doyle⁷ have reported the electron-irradiation-induced $E_C - 0.51$ eV level to anneal out below 300 °C while Dalibor *et al.* have shown the He implantation induced $RD5$ to be significantly reduced after a 430 °C annealing.⁴ In the present neutron irradiated sample, this deep level anneals at about 350 °C. The annealing behavior of the $E_C - 0.51$ eV observed in Aboelfotoh and Doyle's study (and also the $E_C - 0.50$ eV level in the present study) is very similar to that of the $T5$ center found in Itoh *et al.*'s EPR study of electron and proton irradiated *p*-type 3C-SiC, which was attributed to a positively charged carbon vacancy V_C^+ .²¹ The $T5$ center was found to anneal out ~ 300 °C. This led that the E_i level is suggested to be related to a carbon vacancy. However, in a more recent EPR study, Son, Hai, and Janzén²² have identified the $E15$ center, which anneals at 500 °C, as a positively charged carbon vacancy V_C^+ , an annealing temperature that coincides with the carbon vacancy as seen from positron lifetime measurements.^{23,24} Son and co-workers further argued the $T5$ is not a V_C^+ defect but possibly a $V_C + nH$ ($n = 1, 2$) complex.²² In summary, the evi-

TABLE II. Energy levels ($E_C - E_i$), capture cross sections (σ_n), and concentrations (N_i) of the deep levels determined using the DLTS data of the neutron irradiated n -type 6H-SiC samples annealed at 1600 °C.

	$E_C - E_i$ (eV)	σ_n (cm ²)	N_i (cm ⁻³)	References
NE1	0.44	$\sim 10^{-15}$	$2-5 \times 10^{14}$	ID6 $E_C - 0.40-0.43$ eV (Ref. 4) BE2 $E_C - 0.44$ eV (Ref. 29)
NE2	0.53	$\sim 10^{-15}$	$4-8 \times 10^{14}$	ID7 $E_C - 0.50-0.54$ eV (Ref. 4) BE3 $E_C - 0.53$ eV (Ref. 29)
NE3	0.64	$\sim 10^{-16}$	$1-3 \times 10^{14}$	
NE4	0.68	$\sim 10^{-17}$	$2-6 \times 10^{14}$	

dence strongly points towards E_i being a V_C or a V_C related complex with the possibility of hydrogen association requiring further investigation.

C. E_1/E_2 levels

For the case of the E_1/E_2 ($E_C - 0.36/0.44$ eV) level, the introduction rate and thermal annealing behavior observed on the present neutron irradiated n -type 6H-SiC is markedly different from those observed for electron irradiated samples.⁵⁻⁷ As noted while E_1/E_2 are usually the dominant peaks in the DLTS spectra of electron-irradiated n -type 6H-SiC materials, the relative intensity of E_1/E_2 in the neutron-irradiated material is low (see Fig. 1). Speculation that the relative lower intensity of E_1/E_2 in the neutron-irradiated spectrum is due to the effect of the deep level occupancy, which is determined by the Fermi level position, can be ruled out. First, in the present study, the total concentration of observed deep levels which could act as potential compensating centers was at least one order of magnitude smaller than the dopant concentration. Second, the observation of the ED1 level indicates that the Fermi level is at least high enough to populate the level at $E_C - 0.23$ eV. Third, the low relative intensity is a general consistency with DLTS spectra seen under heavy particle irradiation. More specifically, the observed E_1/E_2 intensity increases with annealing temperature in the present neutron-irradiated samples becoming dominant at 500 °C and persisting until annealing temperatures of 1200 °C. The observation of similar increasing and subsequent decreasing behavior, together with a similarly relatively low E_1/E_2 intensity, is also seen in other n -type 6H-SiC samples irradiated with heavy particles, like He (Ref. 4) or deuterium.⁷ For He and deuterium irradiated samples, the E_1/E_2 peak is found to be dominant at the annealing temperatures of 430 and 800 °C, respectively.^{4,7}

The microstructure of E_1/E_2 is still not yet confirmed with possible suggestions being the negatively charged carbon vacancy V_C ,⁷ a divacancy $V_C V_{Si}$,⁶ or a complex consisting of a V_{Si} .^{25,26} Other than these suggestions, one clue to the possible identity of the E_1/E_2 defect comes from the work of Lingner, Greulich-Weber, and Spaeth¹⁸ who have studied neutron irradiated n -type 6H-SiC sample with electron paramagnetic resonance (EPR), magnetic circular dichroism of the absorption (MCDA) and MCDA detected EPR (MCDA-EPR). $P6/P7$ centers were detected only in neutron irradiated samples after a 600 °C annealing, but not in the un-irradiated or the as-irradiated samples. The $P6/P7$

signal was found to persist at 1200 °C annealing. Theoretical modeling performed by these authors showed the carbon antisite carbon vacancy $C_{Si}V_C$ center to be the only simple structure capable of producing the observed optical transitions and it was proposed that $C_{Si}V_C$ forms through the reaction $V_{Si} + C_C \rightarrow C_{Si}V_C$ during the annealing process. The observation made in the neutron irradiated n -type 6H-SiC materials that, the intensities of the deep levels E_1/E_2 and the $P6/P7$ centers were small in the un-irradiated or the as-irradiated samples but increased after the 600 °C annealing could thus be possibly explained if E_1/E_2 and $P6/P7$ originated from the same defect $C_{Si}V_C$.

As the E_1/E_2 intensities keep on increasing in the range of annealing temperatures up to 500 °C and reach the maximum at this temperature, we would point out that if $C_{Si}V_C$ is responsible for E_1/E_2 it is unlikely that these sites are all created from the mobility and annihilation of a V_{Si} since the silicon vacancy is known to be stable in the temperature range up to ~ 700 °C. For example, using the positron lifetime technique, Ling, Beling, and Fung²³ have observed that V_{Si} related defect in n -type 6H-SiC anneals only after 650 °C annealing. Moreover, Sörman *et al.*²⁷ have noted the stability of photoluminescence (PL) lines associated with the isolated silicon vacancy, up to 750 °C. It is more likely that there exists another channel that the $C_{Si}V_C$ defect could form through. Since the V_C related defect is mobile in the temperature below 500 °C (see discussed on E_i level above), one of the possible formation reactions is through the process $V_C + C_{Si} \rightarrow C_{Si}V_C$, since it is known that the carbon antisite has low formation energy, which is likely to be the most common native defect in as-grown SiC.²⁸ Such a formation is consistent with the observation that the decrease of the E_i annealing curve coincides well with the increase of the E_1/E_2 intensities [Figs. 3 and 4(a)]. While looking promising, the identification of E_1/E_2 with $C_{Si}V_C$ is not unambiguously proved and further investigations are certainly needed for further clarification.

D. Z_1/Z_2 and NE3/NE4 levels

Earlier thermal annealing studies indicated that the Z_1/Z_2 centers persisted at annealing temperatures up to 1700 °C,^{2,3} in contradiction with the present study which shows the levels to have completely annealed out by 900 °C and other recent results showing that the Z_1/Z_2 deep levels disappear at temperatures below 1000 °C.^{6,7} The early study can be explained from the observation in the present study,

that as the Z_1/Z_2 levels anneal so two new deep level centers ($NE3$ and $NE4$) having very close ionization energies to those of Z_1/Z_2 are generated upon the 1600 °C annealing. It is thus possible that the deep levels termed Z_1/Z_2 reported stable up to 1700 °C in the earlier study are indeed the $NE3/NE4$ annealing induced deep levels defects. To support this view we point out that under the same rate window settings the peak position temperatures of the $NE3$ and $NE4$ deep levels are about 40 K higher than those of the Z_1/Z_2 levels (Fig. 5), indicating that the capture cross sections for $NE3/NE4$ defects are lower than those of the Z_1/Z_2 centers (as can also be seen from the Arrhenius plots of Fig. 6). Although cross sections can vary greatly for samples with different strain and with different modes of carrier scattering, the different cross sections indicate that the $NE3/NE4$ centers are either a modified form of the Z_1/Z_2 centers or are of a completely different structure. The fact that the 900 °C anneal completely removes Z_1/Z_2 [Fig. 3(c)] also supports the view that the structures responsible for these levels have been removed by annealing and thus that the $NE3/NE4$ levels are of a new origin.

The earlier study that suggested that Z_1/Z_2 was stable up to 1700 °C gave rise to the idea that the defect center could be $V_{Si}V_C$. In view of the above observations that Z_1/Z_2 anneals at the much lower temperature range of 500–900 °C and the fact that this annealing behavior parallels that of the isolated silicon vacancy V_{Si} as seen by positron lifetime spectroscopy^{23,24} and PL²⁷ has led a number of workers to suggest that Z_1/Z_2 is produced by V_{Si} .^{25,26} Moreover, measuring the positron lifetime spectra of irradiated 6H–SiC materials with monochromatic illumination, V_{Si} has been recently shown to have an ionization level at 0.6 ± 0.1 eV below the conduction band, which indeed coincides with that of Z_1/Z_2 .²⁶ This identification can also explain the double peak nature of this level, with one peak coming from the hexagonal-site h and the other from the quasicubic-sites k_1 , k_2 .

E. $NE1$ and $NE2$

The activation energies of the $NE1$ and $NE2$ levels found in the 1600 °C annealed samples are determined at $E_C - 0.44$ and 0.53 eV. Their concentrations are found to be higher on samples annealed at a temperature of 1600 °C than on those annealed at 1400 °C indicating that these peaks are indeed thermally induced. We noted that the activation energy of the $NE1$ level is identical to that of E_1/E_2 . However, as shown in Fig. 5, under the same rate window setting, the temperature position of the $NE1$ peak maximum is shifted to higher temperature by 50 K indicating that $NE1$ is a peak of different microstructural origin. This view is supported by the absence in $NE1$ of the well known overlapping peak structure of E_1/E_2 which has been suggested to result from the same defect on inequivalent 6H–SiC lattice sites. Therefore, these results make it seem unlikely that the $NE1$ originates from the same defect centers causing E_1/E_2 .¹⁰ On the other hand, evidence exists from two other studies that $NE1$ and $NE2$ are to be associated with postimplantation annealing induced deep level centers. First, Dalibor *et al.*⁴

have observed the electron traps labeled $ID6$ and $ID7$ (having activation energies of 0.40–0.43 and 0.50–0.54 eV, respectively) in n -type 6H–SiC samples implanted by vanadium and titanium followed by 30 min 1700 °C annealing. Second, electron traps $BE2$ and $BE3$ with identical activation energies to those of $NE1$ and $NE2$ have also been observed in Be implanted n -type 6H–SiC after annealing at 1600 °C.²⁹ Thus in summary, the close similarity of the activation energies of the $NE1$ (and $NE2$) deep levels observed in the present study with those of $ID6/BE2$ (and $ID7/BE3$) found in high temperature annealed ion implanted n -type 6H–SiC materials (refer to Table II), made it reasonable to suggest that $NE1$ is probably the same level as $ID6/BE2$ and $NE2$ the same level as $ID7/BE3$.

It is also worth pointing out that $NE1$ – $NE4$ can also be observed in the 1600 °C annealed un-irradiated sample, despite the fact that their intensities are much lower than those in the neutron-irradiated sample. As these four peaks are not found in the as-grown sample (DLTS measurement performed but not shown), this implies the observed $NE1$ – $NE4$ defects are the products of the thermal annealing. As the neutron irradiation enhances the formation of these defects, it implies some of the neutron-irradiation induced defects are possibly involved in the reaction that leads to the formation of $NE1$ – $NE4$.

V. SUMMARY

In summary, DLTS has been used to study deep level defects in n -type 6H–SiC materials induced by neutron irradiation. Additional isochronal annealing has also been performed in order to characterize the induced defects. Deep levels at $E_C - 0.23$ eV ($ED1$), $E_C - 0.36/0.44$ eV (E_1/E_2), $E_C - 0.50$ eV (E_i or $RD5$), and $E_C - 0.62/0.68$ eV (Z_1/Z_2) have been identified and studied. $ED1$ and E_i were observed to anneal out at relatively low temperatures (below 350 °C). It has been suggested that the structure of E_i is likely to be V_C related. Unlike the electron irradiated material, but similar to He and deuterium implanted, the E_1/E_2 are found not to be the dominant peaks in as-neutron-irradiated DLTS spectra. The fact that the intensity of increased E_1/E_2 first increases with annealing temperature, reaching a maximum at 500–750 °C and then annealing out at 1400 °C, has been tentatively interpreted, together with other evidence, in terms of the $C_{Si}V_C$ center. The Z_1/Z_2 levels were found to anneal out at temperatures below 900 °C, while strongly suggesting that the V_{Si} defect for the responsible microstructure does not rule out other defect centers.

An important observation made in the present work has been that of the thermal generation of deep levels $NE1$ – $NE4$ at annealing temperatures above 1400 °C. The evidence that we have given strongly suggests that these levels are not to be associated with either E_1/E_2 or Z_1/Z_2 but are indeed new defect levels happening to have very similar energy levels. While these new levels may be associated with microstructures very similar in some way to those responsible for E_1/E_2 or Z_1/Z_2 , it is also possible that their origin could have no association with the origin of the E_1/E_2 or Z_1/Z_2 levels. It is too early to speculate on the origin of

$NE1-NE4$, but it is hoped that the evidence given that these defects are indeed different than E_1/E_2 or Z_1/Z_2 will stimulate further research into their microscopic origin.

ACKNOWLEDGMENTS

The work described in this article is partially supported by a grant from the Research Grant Council of the Hong Kong Special Administrative Region, China (under Project Nos. 7085/01P, HKU1/00C, HKU7137/99P and HKU7103/02P) and the Hung Hing Ying Physical Science Research Fund. One of the authors (X.D.C.) wishes to acknowledge his PDF support from HKU. M. G. also acknowledges support from the grant of National Nature Science of China (No. 60076010).

- ¹H. Morkoç, S. Strite, G. B. Gao, M. E. Lin, B. Sverdlov, and M. Burns, *J. Appl. Phys.* **76**, 1363 (1994).
- ²G. Pensl and W. J. Choyke, *Physica B* **185**, 264 (1993).
- ³H. Zhang, G. Pensl, A. Dornen, and S. Leibenzeder, *Journal of the Electrochemical Society, Extended Abstracts* **89-2**, 699 (1989).
- ⁴T. Dalibor, G. Pensl, H. Matsunami, T. Kimoto, W. J. Choyke, A. Schoener, and N. Nordell, *Phys. Status Solidi A* **162**, 199 (1997).
- ⁵C. G. Hemmingsson, N. T. Son, O. Kordina, E. Janzén, and J. L. Lindström, *J. Appl. Phys.* **84**, 704 (1998).
- ⁶M. Gong, S. Fung, C. D. Beling, and Z. You, *J. Appl. Phys.* **85**, 7604 (1999).
- ⁷M. O. Aboelfotoh and J. P. Doyle, *Phys. Rev. B* **59**, 10 823 (1999).
- ⁸A. A. Lebedev, A. I. Veinger, D. V. Davydov, V. V. Kozlovski, N. S. Savkina, and A. M. Strel'chuk, *J. Appl. Phys.* **88**, 6265 (2000).
- ⁹Th. Frank, G. Pensl, Song bai, R. P. Devaty, and W. J. Choyke, *Mater. Sci. Forum* **338-342**, 753 (2000).

- ¹⁰M. Weidner, T. Frank, G. Pensl, A. Kawasuso, H. Itoh, and R. Krause-Rehberg, *Physica B* **308-310**, 633 (2001).
- ¹¹H. Heissenstein, C. Peppermüller, and R. Helbig, *J. Appl. Phys.* **83**, 7542 (1998).
- ¹²A. I. Veinger, A. G. Zabrodshi, G. A. Lomakina, and E. N. Mokhov, *Sov. Phys. Solid State* **28**, 917 (1986).
- ¹³V. Nagesh, J. W. Farmer, R. F. Davis, and H. S. Kong, *Radiat. Eff. Defects Solids* **112**, 77 (1990).
- ¹⁴V. Nagesh, J. W. Farmer, R. F. Davis, and H. S. Kong, *Appl. Phys. Lett.* **50**, 1138 (1987).
- ¹⁵A. I. Veinger, A. A. Lepneva, G. A. Lomakina, E. N. Mokhov, and V. I. Sokolov, *Sov. Phys. Semicond.* **18**, 1256 (1984).
- ¹⁶M. Okada, K. Atobe, M. Nakagawa, S. Kanazawa, I. Kanno, and I. Kimura, *Nucl. Instrum. Methods Phys. Res. B* **166, 167**, 399 (2000).
- ¹⁷N. Nayashi, H. Watanabe, K. Sakai, K. Kuriyama, Y. Ikeda, H. Maekawa, and T. Miura, *Mater. Sci. Forum* **196-201**, 1243 (1995).
- ¹⁸Th. Lingner, S. Greulich-Weber, and J. M. Spaeth, *Phys. Rev. B* **64**, 245212 (2001).
- ¹⁹C. V. Reddy, S. Fung, and C. D. Beling, *Rev. Sci. Instrum.* **67**, 257 (1996).
- ²⁰D. V. Lang, *J. Appl. Phys.* **45**, 3023 (1974).
- ²¹H. Itoh, A. Kawasuso, T. Ohshima, M. Yoshikawa, I. Nashiyama, S. Tanigawa, S. Misawa, H. Okumura, and Y. Yoshida, *Phys. Status Solidi A* **162**, 173 (1997).
- ²²N. T. Son, P. N. Hai, and E. Janzén, *Phys. Rev. B* **63**, 201201 (2001).
- ²³C. C. Ling, C. D. Beling, and S. Fung, *Phys. Rev. B* **62**, 8016 (2000).
- ²⁴A. Polity, S. Huth, and M. Lausmann, *Phys. Rev. B* **59**, 10603 (1999).
- ²⁵A. Kawasuso, F. Redmann, R. Krause-Rehberg, T. Frank, M. Weidner, G. Pensl, P. Sperr, and H. Itoh, *J. Appl. Phys.* **90**, 3377 (2001).
- ²⁶S. Arpiainen, K. Saarinen, P. Hautojärvi, L. Henry, M. F. Barthe, and C. Corbel, *Phys. Rev. B* **66**, 075206 (2002).
- ²⁷E. Sörman, N. T. Son, W. M. Chen, O. Kordina, C. Hallin, and E. Janzén, *Phys. Rev. B* **61**, 2613 (2000).
- ²⁸L. Torpo, S. Pöykkö, and R. M. Nieminen, *Phys. Rev. B* **57**, 6243 (1997).
- ²⁹X. D. Chen, S. Fung, C. D. Beling, M. Gong, T. Henkel, H. Tanoue, and N. Kobayashi, *J. Appl. Phys.* **88**, 4558 (2000).